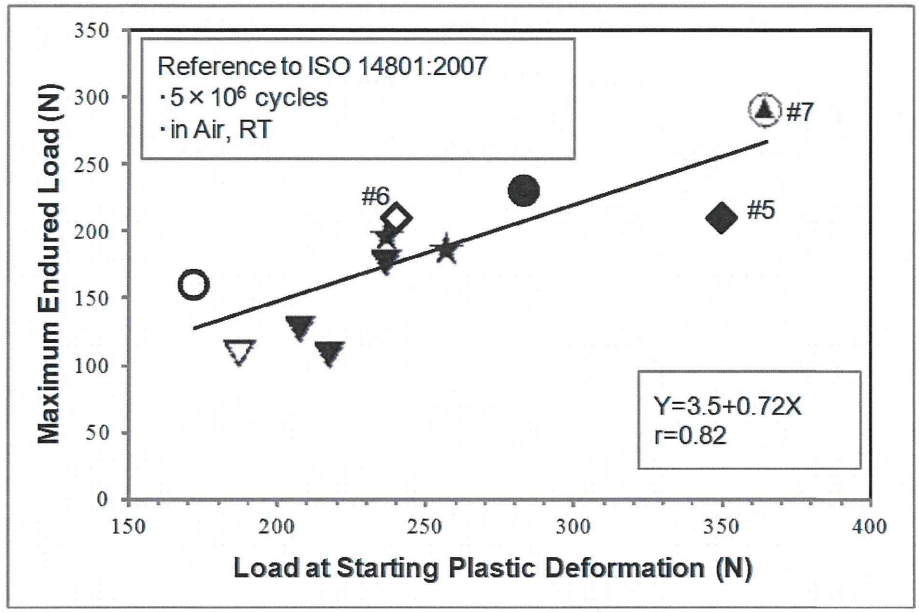

	Implant body		Abutment	
	Joint type	Material	Abutment type	Material
▲	Internal	Ti6AL4V	Screw retain, 30 deg.	Ti6AL4V
●	Internal	Ti6AL4V	Cement retain, 15 deg.	Ti6AL4V
◆	Internal	Ti6AL4V	Screw retain, 0 deg.	Ti6AL4V
★	Internal	Ti6AL4V	Cement retain, 0 deg.	Ti6AL4V
▼	Internal	Ti6AL4V	Abutment for over denture	Ti6AL4V
◇	Internal	cp-Ti	Screw retain, 0 deg.	Ti6AL4V
○	Internal	cp-Ti	Cement retain, 15 deg.	cp-Ti
▽	Internal	cp-Ti	Abutment for over denture	Ti6AL4V

図 1　ISO 14801:2007 に準拠した疲労試験における塑性変形開始荷重と最大耐久荷重との相関

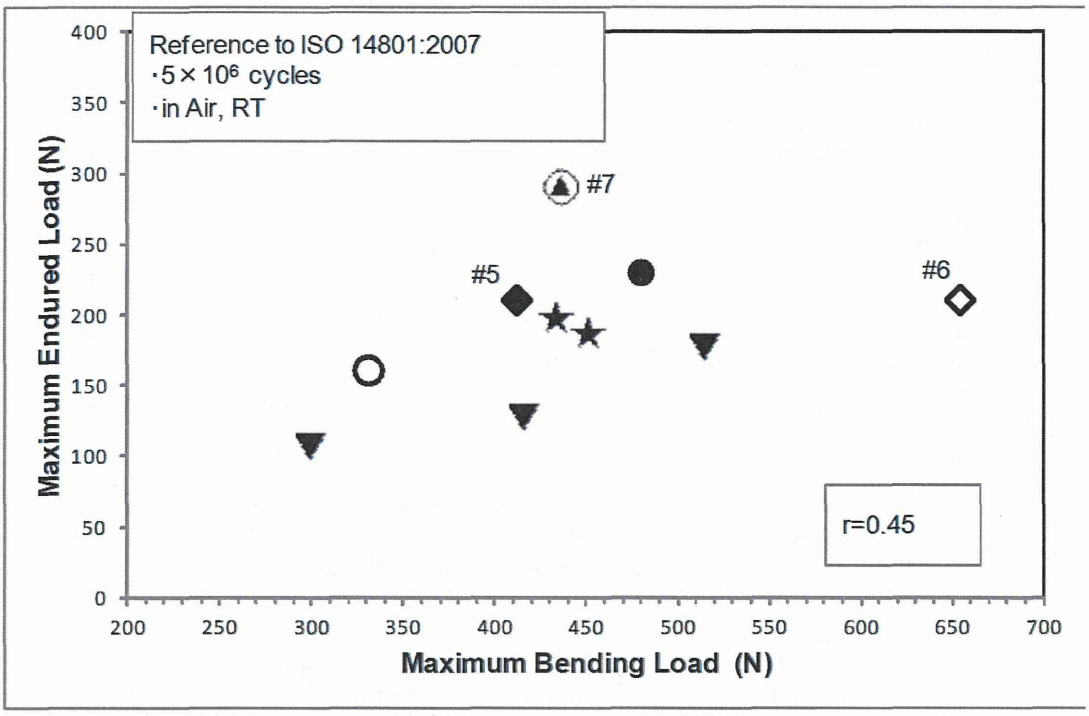

	Implant body		Abutment	
	Joint type	Material	Abutment type	Material
▲	Internal	Ti6AL4V	Screw retain, 30 deg.	Ti6AL4V
●	Internal	Ti6AL4V	Cement retain, 15 deg.	Ti6AL4V
◆	Internal	Ti6AL4V	Screw retain, 0 deg.	Ti6AL4V
★	Internal	Ti6AL4V	Cement retain, 0 deg.	Ti6AL4V
▼	Internal	Ti6AL4V	Abutment for over denture	Ti6AL4V
◇	Internal	cp-Ti	Screw retain, 0 deg.	Ti6AL4V
○	Internal	cp-Ti	Cement retain, 15 deg.	cp-Ti

図 2　ISO 14801:2007 に準拠した疲労試験における最大曲げ荷重と最大耐久荷重との相関

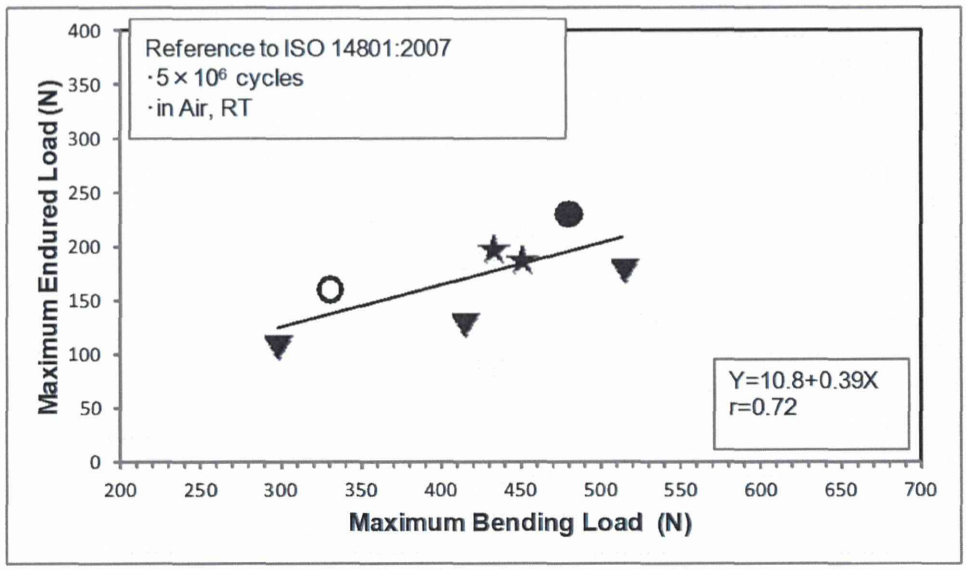

	Implant body		Abutment	
	Joint type	Material	Abutment type	Material
●	Internal	Ti6AL4V	Cement retain, 15 deg.	Ti6AL4V
★	Internal	Ti6AL4V	Cement retain, 0 deg.	Ti6AL4V
▼	Internal	Ti6AL4V	Abutment for over denture	Ti6AL4V
O	Internal	cp-Ti	Cement retain, 15 deg.	cp-Ti

図 3　スクリュー締結式アバットメント付きのデータを除いた最大曲げ荷重と最大耐久荷重との相関

“ワーストケース”選定のためのフローチャート案（ISO 14801 準拠）

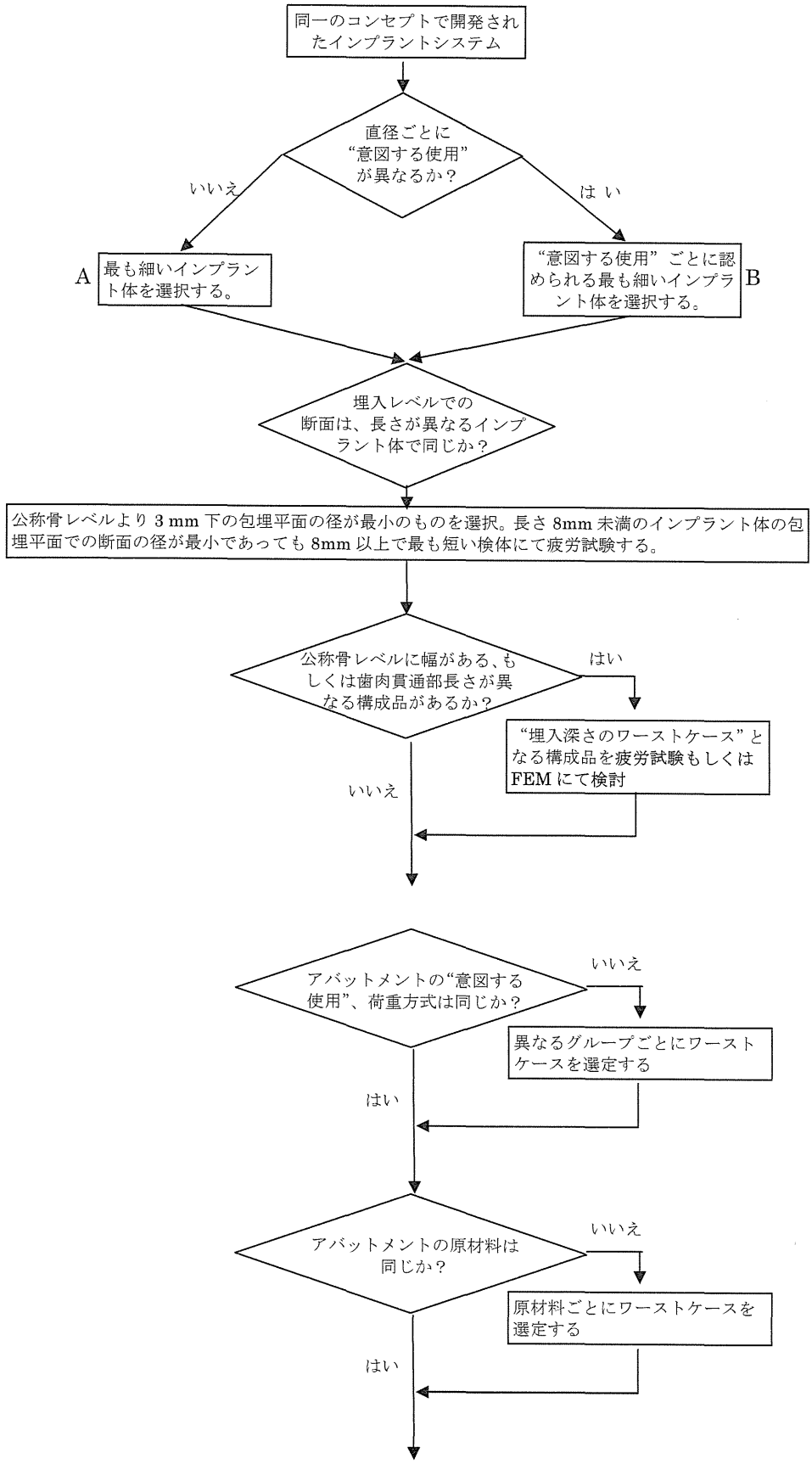

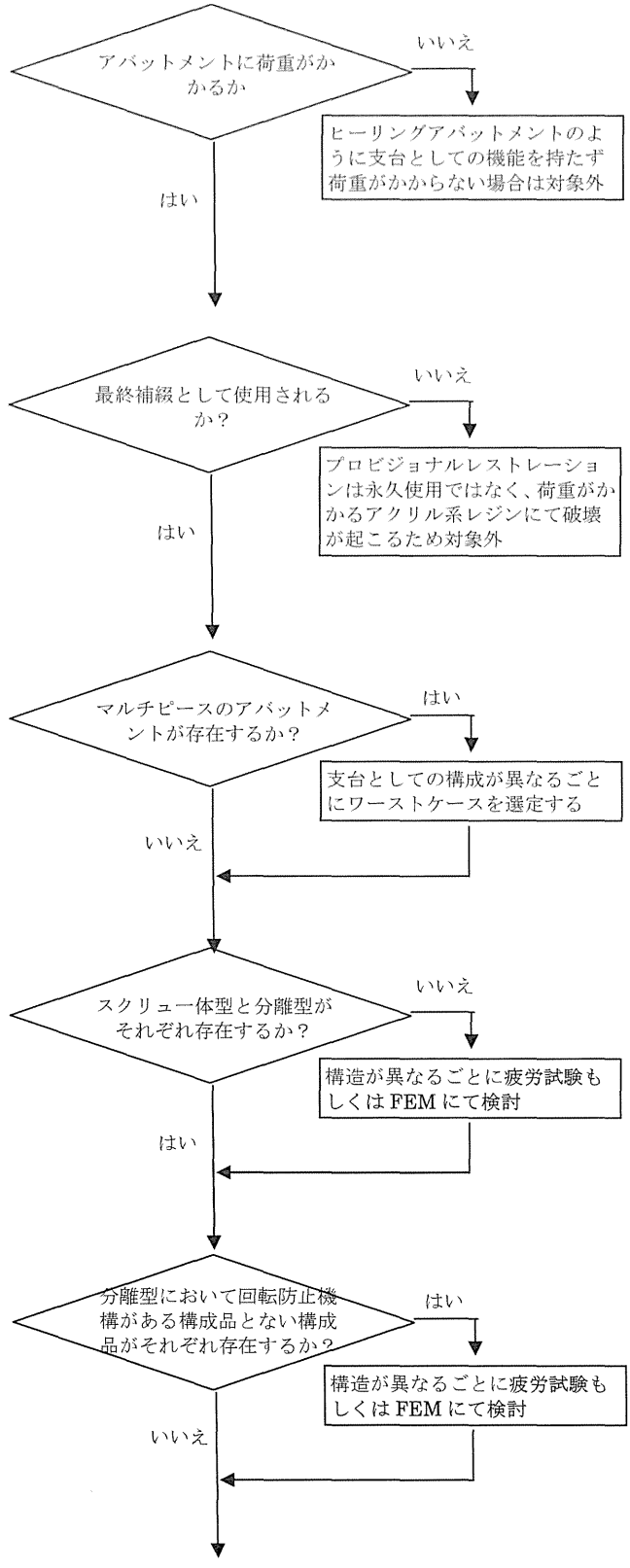
アバットメントのグルーピング
アバットメントに荷重がかかるか
いいえ
ヒーリングアバットメントのように支台としての機能を持たず荷重がかからない場合は対象外
はい
最終補綴として使用されるか？
いいえ
プロビジョナルレストレーションは永久使用ではなく、荷重がかかるアクリル系レジンにて破壊が起こるため対象外
はい
マルチピースのアバットメントが存在するか？
はい
支台としての構成が異なるごとにワーストケースを選定する
いいえ
スクリュー一体型と分離型がそれぞれ存在するか？
いいえ
構造が異なるごとに疲労試験もしくはFEMにて検討
はい
分離型において回転防止機構がある構成品とない構成品がそれぞれ存在するか？
はい
構造が異なるごとに疲労試験もしくはFEMにて検討
いいえ

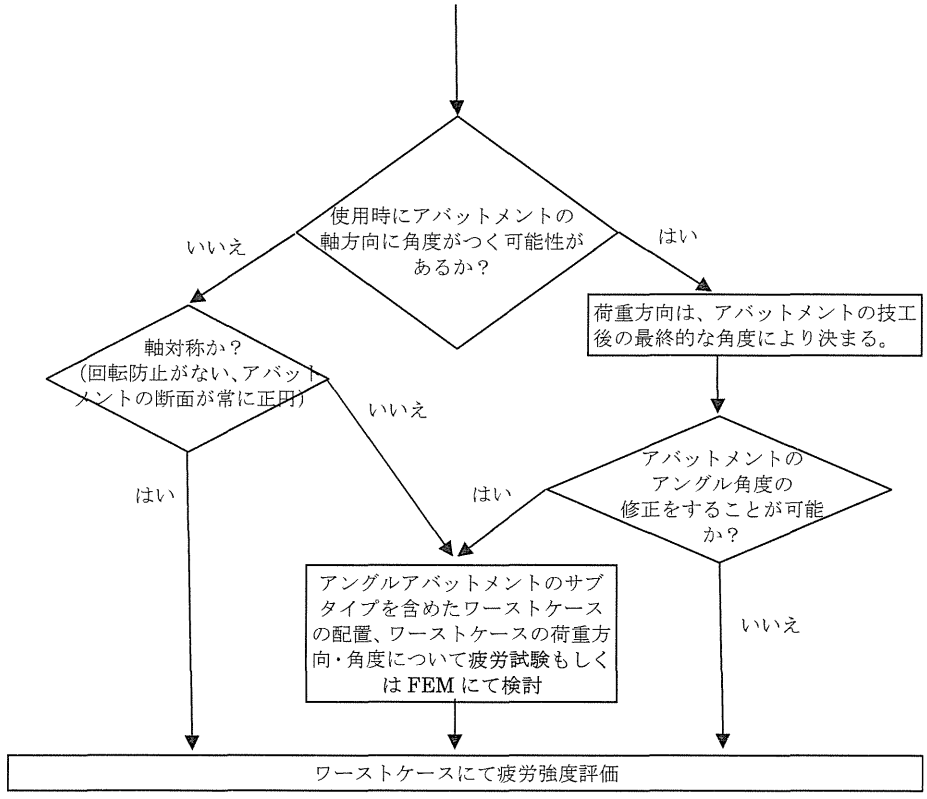
使用時にアバットメントの軸方向に角度がつく可能性があるか？
いいえ
はい
軸対称か？（回転防止がない、アバットメントの断面が常に正円）
いいえ
はい
荷重方向は、アバットメントの技工後の最終的な角度により決まる。
アバットメントのアングル角度の修正をすることが可能か？
はい
いいえ
アングルアバットメントのサブタイプを含めたワーストケースの配置、ワーストケースの荷重方向・角度について疲労試験もしくはFEMにて検討
ワーストケースにて疲労強度評価
アバットメントの配置と荷重方向

分担研究報告書

厚生労働科学研究費補助金

医薬品・医療機器等レギュラトリーサイエンス総合研究事業

「革新的医療機器開発を加速する規制環境整備に関する研究」

分担研究課題名

中間水コンセプトによる新規生体適合性高分子の合成

研究分担者　田中　賢　山形大学大学院理工学研究科バイオ化学工学専攻

研究要旨：本研究では、ポリマー - 水界面に形成される特殊な水和構造（中間水）の発現に関係していると推察されるエーテル結合に注目し、エチレングリコール構造を主鎖または側鎖に導入した新規ポリマーを regio 選択的な開環メタセシス重合法（ROMP）を用いて合成し、得られたポリマーが発現する水和構造と抗血栓性の相関性について検討した。エチレングリコール側鎖長を変更したポリマーでは、エチレングリコールユニット数の増加に伴う中間水量の増加が確認され、ポリマーの一次構造の制御によって中間水量の制御に成功した。

A．研究目的

ポリマー材料を用いた血液接触型医療デバイスには、デバイス表面での血栓形成を防止する抗血栓性が求められている。しかし、ポリマー材料が抗血栓性を発現するメカニズムは解明されていない。我々は、ポリマー - 水界面に形成される特殊な水和構造（中間水）が抗血栓性の発現に寄与しているとの仮説に基づき、ポリマーの一次構造の制御による、水和構造と抗血栓性の制御、およびこれを通じた抗血栓性の発現メカニズムの解明を試みてきた。

本研究では、中間水の発現に関係していると推察されるエーテル結合に注目し、エチレングリコール（EG）構造を主鎖または側鎖に導入した新規ポリマーを regio 選択的な開環メタセシス重合法（ROMP）を用いて合成し（Scheme. 1）、得られたポリマーが発現する水和構造と抗血栓性の相関性について検討を行った。

B．研究方法

モノマーとしてアリル位に3つのEGユニットを有する cyclooctene（COE）誘導体と2 つのメトキシ基をトランス型もしくはシス形で導入した COE 誘導体を合成した。ROMPにより得られたポリマーの主鎖中の二重結合に対して水素添加反応を行い、定序的に側鎖が並んだethyleneとのモデル共重合体を合成した。ポリマーと相互作用する中間水を定量化するために、得られたポリマーを含水させてDSC測定を行なった。また、血小板粘着試験により抗血栓性を確認した。

C．研究結果

モノマーの ROMP によりポリマーを合成した後に、^{1}H-NMR、^{13}C-NMR、2 次元 NMR を用いた構造解析を行行った。側鎖が一定の間隔で導入されたポリマーの生成を確認した（Fig.1）。

EG側鎖長を変更したポリマーでは、EGユニット数の増加に伴う中間水量の増加が見られ、ポリマーの一次構造の制御によっ

て中間水量を制御することができた(Fig.2)。また、多置換体のDSC測定結果から、相互作用する中間水量は立体異性体でおおよそ変わらないことが明らかになった。*t*-PMMは1つのEGユニットを側鎖に有するm=1よりもポリマー鎖の分子運動性が低下する可能性があるため、*t*-PMMの中間水量はm=1よりも減少すると推測していた。*t*-PMMの中間水量を調べたところ、実際にm=1よりも少ない値を示しており、推測通りの結果が得られた。ポリマーの抗血栓性を評価するために、ヒト血小板粘着試験を行なった。EG側鎖長を変更したポリマーでは、EGユニット数の増加に伴った血小板粘着数の減少が見られた。さらに、2つ以上のEGユニットを有するポリマーはPMEAと同程度の血小板粘着数を示していた。また多置換体はm=0とm=1の間の血小板粘着数を示した（Fig.3）。

D．考察

抗血栓性の発現に最も寄与しているポリマー特性を調べるために、血小板粘着数とポリマー特性の相関性について検討した。

ガラス転移温度や液滴法によって得られた接触角の値と血小板粘着数の関係を調べたが、高い相関は得られなかった。ポリマーの主鎖の分子運動性や材料表面の親水性だけではでは抗血栓性の発現について説明できないことがわかった。次に、血小板粘着数と自由水、不凍水、中間水の関係について検討を行った。不凍水量や自由水量に対する血小板粘着数の関係を調べたところ、同じ不凍水量、自由水量を有するポリマーでも血小板粘着数に差が見られた。次に、中間水量と血小板粘着数の相関性について検討した（Fig. 4）。血小板粘着数と中間水量の相関性は他のポリマー特性よりも高く、中間水量の増加に伴った血小板粘着数の減少が見られた。またトランス体は、発現した中間水量から予測されたとおり、目的としていた m=0 と m=1 の間の血小板粘着数を示した。さらに、m=2 の場合でも血小板粘着を PMEA と同程度に抑制していたことから、ポリマー中に中間水量が 0.01 g/g 存在すれば抗血栓性を発現する可能性があることが明らかになった。以上の結果から、中間水量が抗血栓性に与える影響について考察した。中間水が存在しない材料表面では、最表面の不凍水によって吸着タンパク質の構造変化が多く生じ、血小板が多く粘着したと考えられる。しかし、ポリマー中に中間水量が少なくとも 0.01 g/g 存在すれば、タンパク質と不凍水の接触を中間水が防ぐため、吸着タンパク質の構造変化と血小板粘着を抑制したと考えられる（Fig. 5）。

E．結論

本研究ではポリマーの一次構造の制御による、水和構造と抗血栓性の制御に成功し、抗血栓性の発現メカニズムを解明するための新たな知見を得ることができた。

F．研究発表

1.　論文発表

(1) T. Hoshiba, M. Nikaido, M. Tanaka, Characterization of the mechanisms of attachment of tissue-derived cell lines to blood-compatible polymers, *Adv. Healthcare Mater.*, 3, 775-784 (2014).

(2) M.Tanaka, K. Sato, E. Kitakami, S. Kobayashi, T. Hoshiba, K. Fukushima, Design of biocompatible and biodegradable polymers based on intermediate water concept, *Polym. J*, doi:10.1038/pj.2014.129

2.　学会発表

大澤康平,小林慎吾,田中賢,側鎖間隔を制御した新規アミド基導入ポリマーの合成,第63回高分子学会年次大会（2014/5/28-30,名古屋）

戸来奎介,福田考作,小林慎吾,田中賢,側鎖-側鎖間の炭素数を制御した新規 PMEA 類似体の合成とその抗血栓性評価,第 63 回高分子学会年次大会（2014/5/28-30,名古屋）

福田考作,戸来奎介,小林慎吾,田中賢,regio 選択的な開環メタセシス重合による定序性ポリ（3,4-ジメトキシシクロオクテン）の合成とその抗血栓性評価,第 63 回高分子学会年次大会（2014/5/28-30,名古屋）

片岡真依子,岩田幸久,小林慎吾,田中賢,Regio 選択的な開環メタセシス重合を用いた新規 PTHFA 類似体の合成とその血液適合性評価,第 63 回高分子学会年次大会（2014/5/28-30,名古屋）

Meng-Yu TSAI,Yuto INOUE,Takayuki OTA,Kazuki FUKUSHIMA,Masaru TANAKA,DSC Study of Hydrated Aliphatic Carbonyl Polymers,第 63 回高分子学会年次大会（2014/5/28-30,名古屋）

井上裕人,佐藤千香子,佐々木彩乃,福島和樹,田中賢,抗血栓性脂肪族ポリカーボネートの細胞接着性と生分解性,第 63 回高分子学会年次大会（2014/5/28-30,名古屋）

太田貴之,蔡孟諭,福島和樹,田中賢,エーテル置換基を有する環状カルボニル化合物の合成と開環重合,化学系学協会東北大会（2014/9/20-21,米沢）

片岡真依子,岩田幸久,小林慎吾,田中賢,テトラヒドロフラン環を側鎖に有する定序性ポリマーの合成,化学系学協会東北大会（2014/9/20-21,米沢）

大澤康平,小林慎吾,田中賢,側鎖間隔を制御した新規アミド其導入ポリマーの合成とその水和構造解析,化学系学協会東北大会（2014/9/20-21,米沢）

泉井美幸,岩田幸久,小林慎吾,田中賢,Poly(ω‐methoxyalkyl acrylate)類の合成と抗血栓性評価,化学系学協会東北大会（2014/9/20-21,米沢）

甘三奇,小林慎吾,田中賢,水酸基を有するポリ（メタ）アクリレート誘導体の合成とその血液適合性評価,化学系学協会東北大会（2014/9/20-21,米沢）

福島和樹,太田貴之,高岡駿矢,佐藤駿介,松崎広大,岸昂平,有機分子触媒を用いた機能性バイオマテリアルの精密合成,第 63 回高分子討論会（2014/9/24-26,長崎）

福島和樹,蔡孟諭,太田貴之,井上裕人,岸昂平,田中賢,脂肪族エステル系ポリマーの抗血栓性と水和に及ぼす構造因子の解析,第 63 回高分子討論会（2014/9/24-26,長崎）

千場隆志,佐藤一博,大類寿彦,丸山寛花,遠藤千穂,田中賢,中間水が異なる高分子による細胞接着の制御とその応用,第 63 回高分子討論会（2014/9/24-26,長崎）

小林慎吾,福田考作,戸来奎介,北上恵理香,片岡真依子,大澤康平,regioselective ROMP 法を用いた定序性高分子の合成とバイオマテリアルへの応用,第 63 回高分子討論会（2014/9/24-26,長崎）

大澤康平,小林慎吾,田中賢,Regio 選択的な開環メタセシス重合による側鎖間隔を制御した新規アミド基導入ポリマーの合成とその水和構造解析,第 63 回高分子討論会（2014/9/24-26,長崎）

Shenyao Xue, Shingo Kobayashi, Masaru TANAKA, Hiroyuki Furusawa, Measurements of Hydration Amount and Viscoelasticity of Biocompatible Polymers using Quartz-Crystal Microbalance with Dissipation Technique,SmsSys2014（2014/10/15-17,米沢）

大澤康平,小林慎吾,田中賢,Synthesis of Polymers Having Amide Side-chains and Analysis of Hydration Structure,SmsSys2014（2014/10/15-17,米沢）

岸　昂平,井上裕人,佐々木彩乃,佐藤千香子,田中賢,福島和樹,Polymeric Degradable Antimicrobials with Enhanced Blood Compatibility,SmsSys2014（2014/10/15-17,米沢）

田中賢,佐藤一博,北上恵理香,小林慎吾,千場隆志,福島和樹,中間水コンセプトによる生体親和性高分子の設計と診断・治療デバイスへの応用,第23回ポリマー材料フォーラム（2014/11/6-7,奈良）

泉井美幸,岩田幸久,小林慎吾,田中賢,Poly(ω‐methoxyalkyl acrylate)類の合成と抗血栓性評価,第25回バイオマテリアル若手研究会（2014/11/6-7,八王子）

片岡真依子,小林慎吾,田中賢,テトラヒドロフラン環を側鎖に有する定序性高分子の合成と抗血栓性評価,2014 高分子学会東北支部会（2014/11/13-14,郡山）

福島和樹,機能性脂肪族ポリカーボネートを用いたバイオメディカル材料の新展開,2014 高分子学会東北支部会（2014/11/13-14,郡山）

佐藤一博,小林慎吾,綿引省吾,及川昌彦,干場隆志,田中賢,エチレングリコール鎖に注目した Poly(2-methoxyethyl acrylate)類似体の高分子-水相互作用の解析と抗血栓性評価,第 36 回日本バイオマテリアル学会大会（2014/11/17-18,東京）

片岡真依子,小林慎吾,田中賢,テトラヒドロフラン環を側鎖に有する定序性高分子の合成と抗血栓性評価,第 36 回日本バイオマテリアル学会大会（2014/11/17-18,東京）

福田考作,戸来奎介,小林慎吾,田中賢,ポリ（3,4-ジメトキシイクロオクテン）の合成とその抗血栓性評価,第 36 回日本バイオマテリアル学会大会（2014/11/17-18,東京）

泉井美幸,岩田幸久,小林慎吾,田中賢,Poly(ω‐methoxyalkyl acrylate)類の合成と抗血栓性評価,第 36 回日本バイオマテリアル学会大会（2014/11/17-18,東京）

井上裕人,佐藤千香子,佐々木彩乃,福島和樹,田中賢,,抗血栓性を示す生分解性ポリカーボネートを含むポリウレタンの合成と特性評価,第 36 回日本バイオマテリアル学会大会（2014/11/17-18,東京）

太田貴之,蔡孟諭,井上裕人,福島和樹,田中賢,生分解性ポリマーの水和に関与する構造因子の解析と抗血栓性への効果,第 36 回日本バイオマテリアル学会大会（2014/11/17-18,東京）

甘三奇,小林慎吾,田中賢,Water structure of blood compatibe poly[hydroxyalkyl(meth)acrylate]s,第 36 回日本バイオマテリアル学会大会（2014/11/17-18,東京）

戸来奎介,福田考作,小林慎吾,田中賢 ,Synthesis and blood-compatibility evaluation of novel PMEA analogs having precisely placed side-chain branches.,第 10 回 IPC2014（2014/12/2-5,つくば）

片岡真依子,小林慎吾,田中賢,Synthesis of novel polymers having precisely placed tetrahydrofurfuryl side-chain branches via regioselective ring-opening metathesis polymerization and their blood compatibility evaluation, 第 10 回 IPC2014（2014/12/2-5,つくば）

福田考作,小林慎吾,田中賢,Synthesis of sequence- and geometry-specific poly(3,4-dimethoxycyclooctene)s and their antithrombotic evaluation,第 10 回 IPC2014（2014/12/2-5,つくば）

佐藤一博,小林慎吾,綿引省吾,及川昌彦,干場隆志,田中賢,The relationship between water structure and blood compatibility in poly(2poly(2 -methoxyethyl acrylate) (PMEA) analogues,第 10 回 IPC2014（2014/12/2-5,つくば）

福島和樹,井上裕人,岸昂平,太田貴之,Meng-Yu TSAI,佐藤駿祐, 松崎広大,Functional Degradable Biomaterials Based on Organocatalysis and Substituted Cyclic Carbonates,第 10 回 IPC2014（2014/12/2-5,つくば）

小林慎吾,福田考作,戸来奎介,片岡真依子,大澤康平,田中賢,Synthesis of Sequence-specific Polymers via Regioselective ROMP and Biomaterial Applications,第 10 回 IPC2014（2014/12/2-5,つくば）

甘三奇,小林慎吾,田中賢,Synthesis and anti-thrombotic evalution of novel PHEMA analogs having different side-chain structures,第 10 回 IPC2014（2014/12/2-5,つくば）

大澤康平,小林慎吾,田中賢,Synthesis of novel regioregular polymers having amide side-chains via regioselective ring-opening metathesis polymerization and their biocompatibility evaluation,第 10 回　IPC2014（2014/12/2-5,つくば）

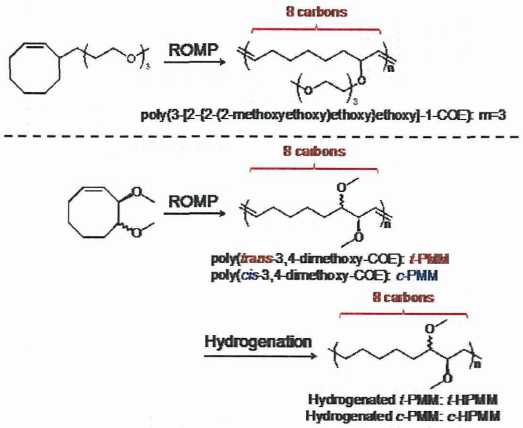

Scheme. 1 ROMPと水素添加反応によるポリマー合成

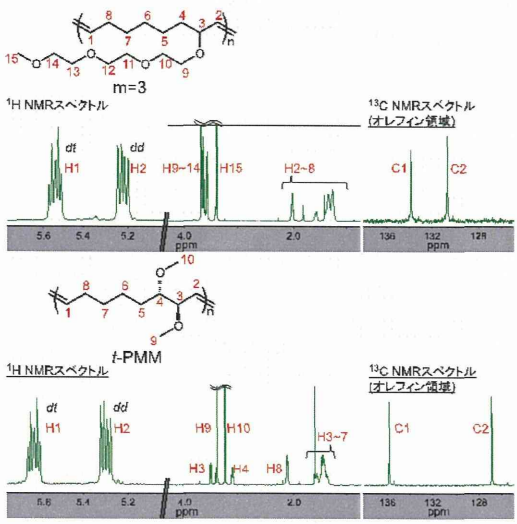

Fig. 1 m=3とt-PMMのNMRの測定結果

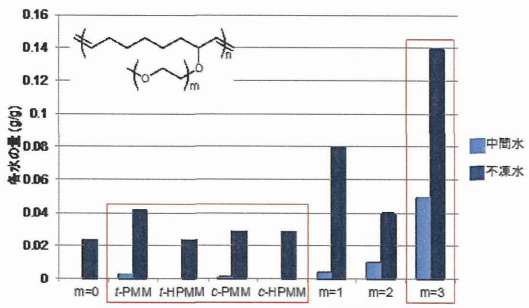

Fig. 2 中間水と不凍水の定量結果

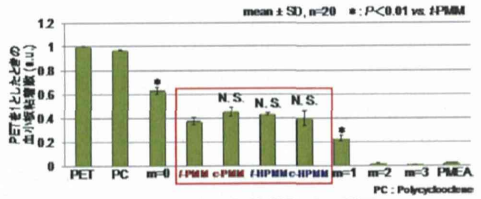

Fig. 3 ヒト血小板粘着試験の結果

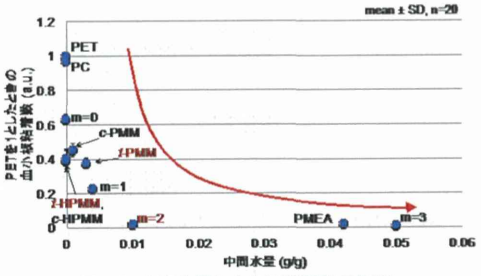

Fig. 4 中間水量と血小板粘着数の関係

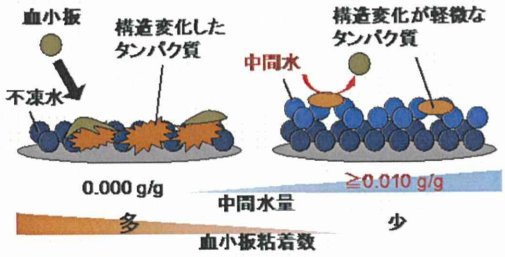

Fig. 5 中間水量が抗血栓性に及ぼす影響

Ⅲ．　研究成果の刊行に関する一覧表

研究成果の刊行に関する一覧表

雑誌

発表者氏名	論文タイトル名	発表誌名	巻号	ページ	出版年
Sakata S, Inoue Y, Ishihara K.	Molecular Interaction Forces Generated during the Protein Adsorption to Well-defined Polymer Brush Surfaces	Langmuir,		dx.doi.org/10.1021/acs.langmuir.5b00351	2015
Sakata S, Inoue Y, Ishihara K.	Nano-scale Molecular Interaction Force Measurement for Analysis of Protein Adsorption on the Surface	Trans. Mat. Soc. Japan,	39	185-188	2014
Shigemitsu R, Yoda N, Ogawa T, Kawata T, Gunji Y, Yamakawa Y, Ikeda K, Sasaki K.	Biological-data-based finite-element stress analysis of mandibular bone with implant-suported overdenture	Comput. Biol. Med,	54	44-52	2014
Hoshiba T, Nikaido M, Tanaka M.	Characterization of the mechanisms of attachment of tissue-derived cell lines to blood-compatible polymers	Adv. Healthcare. Mater,	3	775-784	2014
Tanaka M, Sato K, Kitakami E, Kobayashi S, Hoshiba T, Fukushima K.	Design of biocompatible and biodegradable polymers based on intermediate water concept	Polym. J,	doi:10.1038/pj.2014.129	doi:10.1038/pj.2014.129	2014

Ⅳ.　研究成果の刊行物・別刷り

Langmuir

Article

pubs.acs.org/Langmuir

Molecular Interaction Forces Generated during Protein Adsorption to Well-Defined Polymer Brush Surfaces

Sho Sakata,[†] Yuuki Inoue,*[,†] and Kazuhiko Ishihara*[,†,‡]

[†]Department of Materials Engineering and [‡]Department of Bioengineering, School of Engineering, The University of Tokyo 7-3-1, Hongo, Bunkyo-ku, Tokyo 113-8656, Japan

Supporting Information

ABSTRACT: The molecular interaction forces generated during the adsorption of proteins to surfaces were examined by the force-versus-distance (f–d) curve measurements of atomic force microscopy using probes modified with appropriate molecules. Various substrates with polymer brush layers bearing zwitterionic, cationic, anionic, and hydrophobic groups were systematically prepared by surface-initiated atom transfer radical polymerization. Surface interaction forces on these substrates were analyzed by the f–d curve measurements using probes with the same polymer brush layer as the substrate. Repulsive forces, which decreased depending on the ionic strength, were generated between cationic or anionic polyelectrolyte brush layers; these were considered to be electrostatic interaction forces. A strong adhesive force was detected between hydrophobic polymer brush layers during retraction; this corresponded to the hydrophobic interaction between two hydrophobic polymer layers. In contrast, no significant interaction forces were detected between zwitterionic polymer brush layers. Direct interaction forces between proteins and polymer brush layers were then quantitatively evaluated by the f–d curve measurements using protein-immobilized probes consisting of negatively charged albumin and positively charged lysozyme under physiological conditions. In addition, the amount of protein adsorbed on the polymer brush layer was quantified by surface plasmon resonance measurements. Relatively large amounts of protein adsorbed to the polyelectrolyte brush layers with opposite charges. It was considered that the detachment of the protein after contact with the polymer brush layer hardly occurred due to salt formation at the interface. Both proteins adsorbed significantly on the hydrophobic polymer brush layer, which was due to hydrophobic interactions at the interface. In contrast, the zwitterionic polymer brush layer exhibited no significant interaction force with proteins and suppressed protein adsorption. Taken together, our results suggest that to obtain the protein-repellent surfaces, the surface should not induce direct interaction forces with proteins after contact with them.

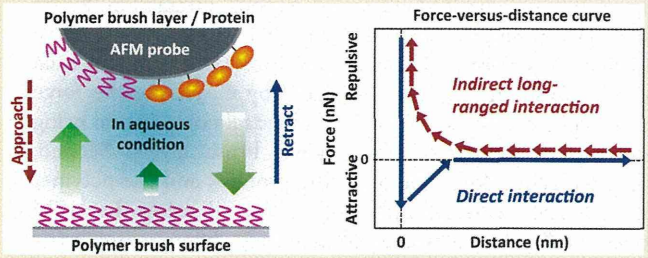

1. INTRODUCTION

A series of biological reactions progresses hierarchically at interfaces between biomolecules and the surface with which they interact. Protein adsorption on the surfaces of materials is an initial reaction and is generally induced immediately. The amount of adsorbed protein and its conformational change are significant factors that determine the subsequent biological responses at cellular and tissue levels.[1−3] Therefore, protein adsorption to surfaces should be completely understood and regulated for developing safer and more efficacious medical devices and maintaining cell function in order to fully achieve regenerative medicine. Protein adsorption depends on various intermolecular/surface interaction forces operating between the material surface and proteins.[4,5] Much research has elucidated protein adsorption behavior in the context of physicochemical surface properties by using the water contact angle or surface ζ-potential as parameters. However, analyses concerning the strength or range of such interaction forces have been relatively limited. The objective of this study was to clarify the protein adsorption process from the perspective of molecular interaction forces operating on surfaces.

Generally, electrostatic and hydrophobic forces are considered to be the main driving forces for protein adsorption on surfaces. However, it is difficult to precisely distinguish these interaction forces in the case of conventional polymeric surfaces or polymer-coated surfaces because of their vague arrangement of polymer chains. Therefore, in the present study we utilized polymer brush surfaces prepared via the surface-initiated atom transfer radical polymerization (SI-ATRP) method.[6−12] In SI-ATRP, monomers are uniformly polymerized from surface-immobilized initiators, which enable the construction of homogeneous polymer layers composed of a single monomer unit on the surfaces of various substrates. Moreover, the surface's physicochemical properties (hydrophilicity/hydrophobicity and surface potential) can be controlled over a wide range by varying the chemical structure of monomer units.[13−15] Thus, the clarification of surface interaction forces would be enhanced by utilizing polymer brush surfaces

Received: January 28, 2015

DOI: 10.1021/acs.langmuir.5b00351
Langmuir XXXX, XXX, XXX−XXX

prepared from systematically selected monomers (for example, zwitterionic, cationic, anionic, and hydrophobic).

Atomic force microscopy (AFM) is used to quantitatively analyze the various molecular interaction forces on surfaces.[16] In the force-measurement mode of AFM, the interaction force operating between the probe and a sample is acquired as a function of the distance between them, generating a force-versus-distance (f–d) curve. Therefore, AFM enables the detection of long-range interactions operating prior to contact between the probe and the sample as well as the direct interaction forces operating after contact. Moreover, various interaction forces can be evaluated by modification of the probe with appropriate molecules, including peptides, proteins, and polymers.[17−20] The combination of fabrication of well-defined polymer brush surfaces and nanoforce analysis by AFM would help clarify our understanding of various interaction forces operating on surfaces. In this study, two types of f–d curve measurements were performed. First, forces operating on each polymer brush surface were evaluated by measuring the force between polymer brush surfaces of identical composition using AFM probes modified with polymer brush layers. Second, direct interaction forces between the proteins and the polymer brush surfaces were quantitatively evaluated using the AFM probes modified with two proteins having different isoelectric points (pI's) and opposite net charges under physiological conditions. Furthermore, the amounts of these proteins adsorbed on the polymer brush surfaces were quantified, and the relationship among surface interaction forces, the surface–protein direct interaction force, and protein adsorption behavior is discussed.

2. EXPERIMENTAL SECTION

2.1. Materials. 2-Methacryloyloxyethyl phosphorylcholine (MPC) was purchased from NOF (Tokyo, Japan), which was synthesized and purified according to a previously reported method.[21] 2-Trimethylammoniumethyl methacrylate chloride (TMAEMA) and 3-sulfopropyl methacrylate potassium salt (SPMA) were purchased from Tokyo Chemical Industry (Tokyo, Japan). n-Butyl methacrylate (BMA) was purchased from Kanto Chemical (Tokyo, Japan). Copper(I) bromide (CuBr) and 2,2′-bipyridyl (Bpy) were purchased from Wako Pure Chemical Industries (Osaka, Japan). Ethyl-2-bromoisobutyrate (EBIB), 4,4′-dinonyl-2,2′-bipyridyl (DNbpy), bovine serum albumin, and chicken egg white lysozyme were purchased from Sigma-Aldrich (St. Louis, MO, USA). Other organic reagents and solvents were commercially available in extra-pure grade and used without further purification. Silicon wafers were purchased from Furuuchi Chemical (Tokyo, Japan); their surfaces were coated with ~10-nm-thick SiO_2 layers.

2.2. Preparation of Polymer Brush Surfaces. Polymer brush layers were prepared on the initiator-immobilized substrates by SI-ATRP using MPC, TMAEMA, SPMA, and BMA according to a previously reported procedure.[22] Briefly, a surface-immobilizing initiator, (10-(2-bromo-2-methyl)propionyloxy)decyltrichlorosilane (BrC10TCS), was synthesized and immobilized on the silicon substrates as previously described.[23] Specific amounts of the monomer, CuBr, and Bpy were dissolved in degassed solvents. Potassium chloride of the same concentration as SPMA (0.50 mol/L) was added to the SPMA solution to enhance the solubility of SPMA. DNbpy was used as the ligand instead of Bpy for the polymerization of BMA. Then, the BrC10TCS-immobilized substrates and EBIB, as the free initiator, were simultaneously placed into the solution to initiate SI-ATRP. Polymerization was performed with stirring at 20 °C for 24 h. The target degree of polymerization (DP, [monomer]/[free initiator] ratio in the feed) was set at 100. The conversion of monomer to polymer was determined by proton nuclear magnetic resonance spectroscopy (^{1}H NMR) (α-300; JEOL, Tokyo, Japan).

The surface elemental composition of the polymer brush surface was determined by X-ray photoelectron spectroscopy (XPS) (AXIS-Hsi; Shimadzu/Kratos, Kyoto, Japan). The thickness of the polymer brush layer was measured by spectroscopic ellipsometry (α-SE; J.A. Woolam, Lincoln, NE, USA) and was determined using the Cauchy layer model with an assumed refractive index of 1.49 at 632.8 nm. The graft density, σ (chains/nm^2), was calculated using the following equation: $\sigma = h\rho N_A/M_n$, where h (nm) is the ellipsometric thickness of the polymer brush layer, ρ (g/cm^3) is the density of the dry polymer, N_A is Avogadro's number, and M_n is the number-average molecular weight of polymer on the surface. M_n was assumed to be the same as the number-average molecular weight of each polymer in the polymerization solution,[24,25] which was estimated from the degree of polymerization determined by the ^{1}H NMR spectrum of each free polymer. The static air contact angle on the polymer brush surface in pure water and phosphate-buffered solution (PBS; pH 7.4, ionic strength (I) = 150 mmol/L) was measured at room temperature by the captive bubble method using a goniometer (CA-W; Kyowa Interface Science, Saitama, Japan). The supplementary angles ($180°-\theta$) of the static air contact angles (θ) are shown for easy comparison with static water contact angles under dry conditions. The ζ-potential of the polymer brush surface was measured with an electrophoretic light-scattering spectrophotometer (ELS-8000; Otsuka Electronics, Osaka, Japan) equipped with a planar sample cell in water containing 10 mmol/L sodium chloride at room temperature. The chemical structures of the polymer brush layers are shown in Figure 1.

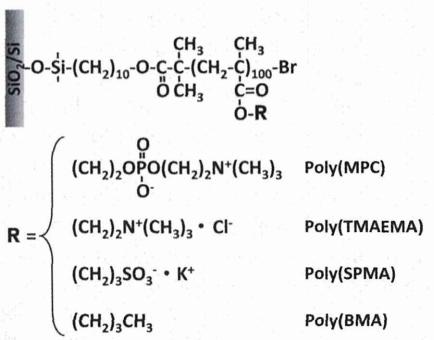

Figure 1. Chemical structures of polymer brush layers.

2.3. Surface Force Analysis. The surface interaction forces at the polymer brush layers were analyzed by f–d curve measurements between polymer brush layers of identical composition (symmetric system) using an AFM equipped with a liquid cell (Nanoscope IIIa; Bruker AXS K.K., Kanagawa, Japan). The essential experimental process is illustrated in Figure 2(a). The polymer brush layers were constructed on the surfaces of silica beads (20 μm diameter, Duke Scientific Co., Palo Alto, CA, USA) using the same method as for the silicon substrates. One silica bead with a polymer brush layer was manually immobilized at the end of a commercial, tipless AFM probe (NP-O; nominal spring constant 0.06 N/m, Bruker AXS K.K.) using a

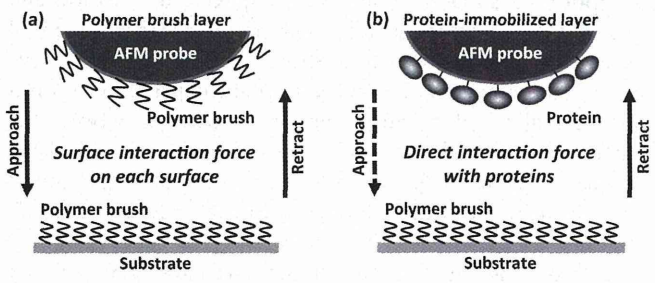

Figure 2. Schematic representation of interaction force measurements by AFM using probes modified with (a) polymer brush layers and (b) a protein-immobilized layer.

DOI: 10.1021/acs.langmuir.5b00351
Langmuir XXXX, XXX, XXX−XXX

small amount of epoxy resin according to a previously reported procedure.[26] The successful immobilization of a silica bead on the probe was confirmed by optical microscopy. The *f*–*d* curve measurement was performed using these probes and the polymer brush substrates, and the *f*–*d* curves on approach and retraction of the symmetric polymer brush surfaces were recorded in aqueous media with different ionic strengths.

2.4. Quantitative Evaluation of Surface–Protein Interaction Forces. The direct interaction force between the proteins and the polymer brush layers was quantitatively evaluated by *f*–*d* curve measurements using an AFM equipped with a liquid cell. The experimental process is illustrated in Figure 2(b). Proteins were chemically immobilized on the surface of the AFM probe (OTR8; nominal spring constant 0.15 N/m, Bruker AXS K.K.) according to a previously reported method.[27] Briefly, 3-nm-thick chromium and sequential 27-nm-thick gold were sputtered on the surface of the probe. The gold-sputtered probe was then immersed in a 1.0 mmol/L solution of 11-mercaptoundecanoic acid in ethanol for 24 h to form a carboxyl-group-terminated self-assembled monolayer on the probe. The carboxyl groups were activated by immersion in an aqueous solution containing *N*-hydroxysuccinimide (50 mmol/L) and 1-ethyl-3-(3-(dimethylamino)propyl)carbodiimide hydrochloride (100 mmol/L). After immersion for 30 min, the probe was rinsed with pure water and immediately immersed in a PBS (pH 7.4, 150 mmol/L) solution of albumin (1.0 mg/mL) or lysozyme (0.10 mg/mL) for 1 h. The immobilization of each protein on the surface was confirmed by XPS and surface plasmon resonance (SPR) (SPR-670M; Moritex, Tokyo, Japan) measurements using gold-sputtered silicon substrates and SPR sensor chips, respectively, instead of the AFM probe. The direct interaction force between the proteins and the polymer brush layers in PBS (pH 7.4, I = 150 mol/L) at room temperature was evaluated from the approaching and retracting traces of the *f*–*d* curve using the protein-immobilized probes. The shift in the deflection value of the retracting trace from the bottom of the retrace line corresponds to the interaction force between the proteins and surfaces. For each measurement, more than 100 approaching/retracting *f*–*d* curves were collected, and the average value was defined as the interaction force between proteins and the polymer brush layers. All measurements were performed at least three times.

2.5. Evaluation of Protein Adsorption Mass. The amount of albumin (pI 4.8) and lysozyme (pI 11.1) adsorbed on the surfaces of polymer brush layers in PBS (pH 7.4, I = 10, 150 mmol/L) at 37 °C was quantified by SPR measurement.[28] The polymer brush layers were prepared on SPR sensor chips by SI-ATRP using 11-(2-bromo-2-methylpropyonyloxy)undecylmercaptan (BUM) as the surface-immobilizing initiator for the thin gold layer on the substrate.[29] A peristaltic pump (Tokyo Rika Kikai, Tokyo, Japan) was used to flow the buffer solution or protein solution through the SPR sensor surfaces at a rate of 500 μL/min. First, a stable baseline signal was established by flowing buffer solution for 10 min. Then, a 1.0 mg/mL protein solution was flowed for 30 min, followed by buffer solution for 10 min to replace the protein solution, wash off the weakly adsorbed proteins from the surface, and re-establish the baseline.

The amount of adsorbed protein, Γ_{SPR} (ng/cm^2), was estimated using the following relationship:[30] $\Gamma_{SPR} = 500 \times \Delta R_{deg}$, where ΔR_{deg} (deg) is the change in the resonance angle before and after protein adsorption. All measurements were performed at least three times.

3. RESULTS AND DISCUSSION

3.1. Characteristics of Polymer Brush Surfaces. In this study, four different types of polymer brush layers, including electrically neutral (zwitterionic), electrolytic (cationic and anionic), and hydrophobic polymers, were prepared to evaluate the various interaction forces generated on these surfaces. The surface elemental composition of the polymer brush layer was evaluated by XPS (XPS spectra are shown in Figure S1 of the Supporting Information). Every polymer brush layer had corresponding elemental peaks expected from the chemical structure of the monomers. Thus, we confirmed that the surface of the substrate was covered with the polymer brush layer. The physicochemical properties of the polymer brush layers are summarized in Table 1. The graft density (density of the polymer chains in a polymer brush layer) of these polymer brush layers was sufficiently high to form a high-density polymer brush structure.[6] The air contact angles on the polymer brush layers in pure water were below 20° for the poly(MPC), poly(TMAEMA), and poly(SPMA) brush layers. That is, these polymer brush layers exhibited a superhydrophilic nature in an aqueous environment. The hydrophilicities of these surfaces were virtually identical regardless of the ionic strength of the medium. In the case of the poly(BMA) brush layer bearing hydrophobic groups, the air contact angle was approximately 75° and did not depend on the ionic strength, which is consistent with its relatively hydrophobic characteristics. The surface ζ-potential values reflected the charge properties of the side chains of each polymer brush layer. That is, the cationic poly(TMAEMA) brush layer had a large positive value whereas the anionic poly(SPMA) brush layer had a large negative value. The poly(MPC) brush layer with zwitterionic phosphorylcholine groups had an almost neutral value. As described above, we confirmed that the systematic model surfaces were prepared from the perspective of the physicochemical surface properties.

Table 1. Physicochemical Properties of Polymer Brush Layers

polymer brush layer	graft density (chains/nm^2)	contact angle of air (deg) in water	contact angle of air (deg) in PBS	ζ-potential (mV)
poly(MPC)	0.33	9 ± 2	9 ± 1	−5.9 ± 2.1
poly(TMAEMA)	0.45	17 ± 0	14 ± 0	64.9 ± 3.6
poly(SPMA)	0.55	13 ± 2	12 ± 1	−74.0 ± 11.7
poly(BMA)	0.75	73 ± 3	74 ± 1	−37.2 ± 6.1

3.2. Surface Interaction Force. To clarify the surface interaction forces on each of the polymer brush surfaces, *f*–*d* curve measurements between polymer brush layers of identical composition were performed with a focus on the approaching and retracting processes. Figure 3 shows the representative *f*–*d* curves recorded for the approaching process of the symmetric poly(MPC), poly(TMAEMA), and poly(SPMA) brush layers. The same procedure was repeated with different ionic strengths of the medium. On the zwitterionic poly(MPC) brush layer, only weak repulsive forces were detected, and these forces were independent of the ionic strength in solution. That is, a specific interaction force was not detected on the poly(MPC) brush layer. On the cationic poly(TMAEMA) and the anionic poly(SPMA) brush layers, strong repulsive forces were detected at long distances in pure water. The strength and range of these forces decreased with increasing ionic strength in solution. Therefore, these repulsions were mainly derived from electrostatic forces. We conclude that electrostatic interactions were predominantly operating on the poly(TMAEMA) and the poly(SPMA) brush layers. It is well known that the charge effects of polyelectrolytes in aqueous media are shielded by the addition of salt. The same phenomenon was observed at the polymer brush layer. Figure 4 shows the representative *f*–*d* curves recorded for the retracting process of the symmetric poly(MPC), poly(TMAEMA), and poly(SPMA) brush layers

DOI: 10.1021/acs.langmuir.5b00351
Langmuir XXXX, XXX, XXX–XXX

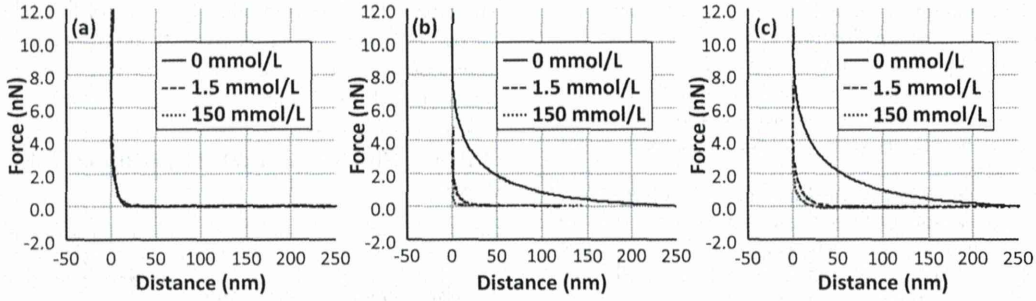

Figure 3. Force versus distance curves recorded for the approaching process between symmetric polymer brush layers of (a) poly(MPC), (b) poly(TMAEMA), and (c) poly(SPMA) in aqueous media with various ionic strengths.

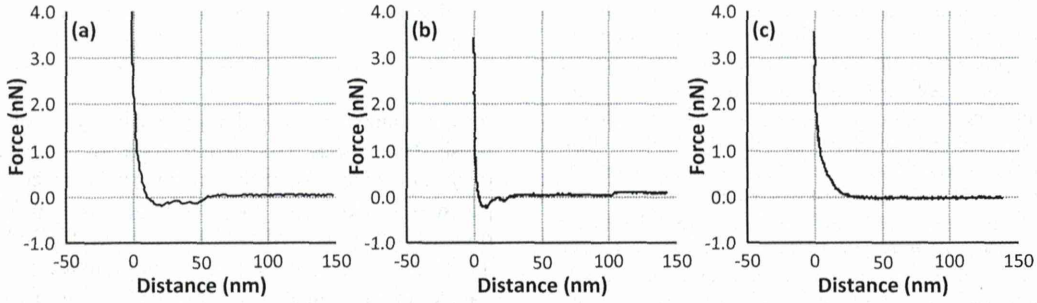

Figure 4. Force versus distance curves recorded for the retracting process between symmetric polymer brush layers of (a) poly(MPC), (b) poly(TMAEMA), and (c) poly(SPMA) in PBS (pH 7.4, I = 150 mmol/L).

in PBS (pH 7.4, I = 150 mmol/L). Interaction forces were not detected when the two identical polymer brush layers were detached. This also indicated that other interactions such as hydrophobic forces did not affect these surfaces under this condition. Figure 5 shows the representative f–d curves

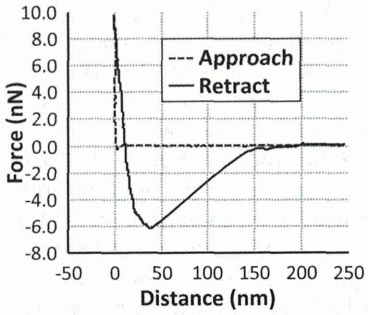

Figure 5. Force versus distance curves recorded on approach and retraction for symmetric poly(BMA) brush layers in PBS (pH 7.4, I = 150 mmol/L).

recorded for the approach and retraction of the symmetric poly(BMA) brush layer in PBS (pH 7.4, I = 150 mmol/L). Although repulsive or attractive forces were not detected when the two layers approached each other, a strong attractive force was detected when the two layers were detached. We conclude that this attraction originated from hydrophobic interactions.[31−33] Hydrophobic interactions between hydrophobic compounds are spontaneously generated in aqueous media due to strong hydrogen bonding among water molecules, which results in the formation of clathrate structures. When hydrophobic compounds interact in aqueous environments, enthalpy increases because some of the clathrate-forming hydrogen bonds between water molecules are broken. According to the Gibbs free energy equation, small positive enthalpy and large negative entropy result in a negative free energy. That is, hydrophobic molecules associate and are stabilized. We believe that this study is the first to detect the hydrophobic interaction force directly and clearly.

In summary, these results show that only electrostatic interactions operated on the cationic poly(TMAEMA) and anionic poly(SPMA) brush layers and only hydrophobic interactions operated on the hydrophobic poly(BMA) brush layer, whereas no specific interaction existed on the zwitterionic poly(MPC) brush layer. That is, interaction forces were clearly separated by utilizing these systematically fabricated polymer brush layers.

3.3. Direct Interaction Force with Proteins. The process of protein adsorption on a material surface is mainly divided into two steps. First, proteins directly interact with the material surface, and an adsorbed protein monolayer is formed. Second, proteins in solution interact with the preadsorbed protein layer, which leads to the formation of an adsorbed protein multilayer. In this respect, the first direct interaction between proteins and surfaces would be critical. Therefore, we quantitatively evaluated the direct interaction force between proteins and the polymer brush surfaces by AFM using protein-immobilized probes. To investigate the effect of charge on the surface–protein interaction force, albumin (pI 4.8) with a negative net charge and lysozyme (pI 11.1) with a positive net charge were used as model proteins in this study.

Before measuring the interaction force between the proteins and the polymer brush surfaces, the immobilization of each protein was carried out on gold-sputtered substrates and SPR sensor chips under the same conditions as those used for the immobilization to the AFM probe to confirm the reaction by XPS and SPR measurement. The XPS spectra indicated the existence of protein-specific atoms, such as carbon, nitrogen, and oxygen (data not shown). The SPR measurements indicated that the amounts of immobilized albumin and lysozyme were ~170 and ~190 ng/cm^2, respectively. These values are comparable to the theoretical values of side-on

DOI: 10.1021/acs.langmuir.5b00351
Langmuir XXXX, XXX, XXX–XXX